STRUCTURAL ANALYSIS OF MINI POWER WEEDER WORM GEAR WITH THREE DIFFERENT MATERIALS

[1]ZAW HTET WIN, [2]WAR WAR MIN SWE, [3]AUNG KO LATT

[1,2,3]Mechanical Engineering Department Mandalay Technological University
E-mail: [1]zawhtetwin1991@gmail.com, [2]warwarminswe288@gmail.com, [3]dr.aungkolat@gmail.com

Abstract - This paper studies about the design and static structural analysis of worm gear in mini power weeder. Mainly, Lewis bending stress is affected on the face of worm gear with tangential force and bending moment is the next consider point for shear stress. Through that, von-Mises stress and effective strain are calculated under bending stress analysis of worm gear by theoretically. A 2.5 hp engine power and 6000 rpm worm speed mini power weeder is used in this paper to do worm gear bending stress analysis. AutoCAD 2019 software is used to model of worm gear and ANSYS 16.2 software is used to analyze static structural analysis of worm gear due to loading condition, with material properties of phosphor bronze, aluminum bronze, and tin bronze in this paper to find out the suitable material of worm gear for good performance. For the phosphor bronze material, the lowest von-Mises stress and effective strain are obtained. Thus phosphor bronze is found to be the suitable material for worm gear.

Keywords - Mini Power Weeder, Worm Gear, Static Structural Analysis, Lewis Bending Stress, Phosphor Bronze.

I. INTRODUCTION

Agriculture is the main industry in Myanmar. 70 percent of the country's population live in rual areas and their livelihood drives the agriculture sector as an important growth engine of rual development.In modern days, industry farming is a way to make easier for their workplace than before. As a result, farm machinery has been progressed in many places of the world. Within many agricultural use, mini power weeder is useful for even those people who use for home gardening because this is very easy and comfortable.

The main parts of mini power weeder are drive shaft, worm and worm gear, and weeder blade. In mini power weeder, the drive shaft forms a direct link between the engine and gear drive assembly. Worm and worm gear design play an important role for transmission system in mini power weeder. Worm gear consists of worm and worm wheel.

Worm gears are used when large speed reductions are required. It can give velocity ratio as high as 300:1 or more in a single step in a minimum of space. Blades are the main part of mini power weeder which are directly engaged with the soil for harvesting the weed from root and loosening of upper layer soil.

In 2018, May Phyoe Thu studied contact stress analysis of stainless steel spur gear by theoretical method using Hertz equation and Finite element analysis using ANSYS 16.0 Workbench [8]. Engr. Rufus O. Chime presented static structural analysis of worm gear by using CAD (Computer-Aided-Design) simulation [9].

Fig.1.shows the assembly of worm and worm gear in mini power weeder. The specification data for worm and worm gear of mini power weeder are obtained from "Farm Machinery Factory, Mandalay Industrial Zone".



Fig.1. Assembly of Worm and Worm gear

II. METHODOLOGY

There are three steps to solve the machinery breakdown because of the gear failure. The first step is design and stress calculation of worm and worm gear by theoretically. The second step is modelling the worm gear with AutoCAD 2019 software. The third step is static structural analysis with ANSYS 16.2 software.

2.1. Design Consideration of Worm and Worm Gear

In designing worm and worm gear, the quantities like engine power, worm speed, face length of worm, and center distance between the shafts are used as specification data which is shown in Table 1.

Parameters	Symbol	Value	Unit
Engine power	P	2.5	hp
Worm speed	N_w	6000	rpm
Face length of worm	L_w	58	mm
Center distance	C	40	mm

Table1: Specification Data for Worm and Worm Gear

The pitch circle diameter of worm in terms of center distance between the shafts is calculated by using equation 1.

$$D_w = \frac{C^{0.875}}{1.416} = 3P_c \quad (1)$$

The axial pitch of the worm $P_a$is equal to the circular pitch of mating worm gear P_c, when the shafts are at right angles [3].

$$P_c = P_a = \pi m_a \quad (2)$$

Axial module,

$$m_a = \frac{D_w}{3\pi} \quad (3)$$

Pitch circle diameter of worm gear,

$$D_g = m_a n_g \quad (4)$$

Actual pitch circle diameter of worm,

$$D_w = 2C - D_g \quad (5)$$

Axial pitch of worm,

$$P_a = \pi m_a \quad (6)$$

For a single start threads, lead is equal to axial pitch, but for multi starts threads, lead is equal to the product of axial pith and number of starts.

$$L = P_a n \quad (7)$$

Where, P_a = axial pitch

n = number of starts

The lead angle is the angle between the tangent to the thread helix on the pith cylinder and the plane normal to the axis of the worm.

$$\lambda = \tan^{-1}\left(\frac{L}{\pi D_w}\right) \quad (8)$$

Face width of worm gear,

$$b = 2.38P_a + 6.5 \quad (9)$$

Rubbing speed,

$$V_r = \frac{\pi D_w N_w}{\cos\lambda} \quad (10)$$

The coefficient of friction varies with the speed.

$$\mu = 0.025 + \frac{V_r}{18000} \quad (\text{for } V_r > 180\text{m/min}) \quad (11)$$

Angle of friction,

$$\phi_1 = \tan^{-1}\mu \quad (12)$$

Efficiency of worm gearing,

$$\eta = \frac{\tan\lambda}{\tan(\lambda+\phi_1)} \quad (13)$$

Parameters	Symbol	Value	Unit
Axial module	m_a	2	mm
Pitch circle diameter of worm gear	D_g	58	mm
Pitch circle diameter of worm	D_w	22	mm
Axial pitch of worm	P_a	6.283	mm
Lead of worm	L	6.283	mm
Lead angle	λ	5.194	deg
Face width of worm gear	b	21.454	mm
Efficiency of worm gearing	η	65.092	%

Table 2: Result Data for Worm and Worm Gear

2.2. Proportions Consideration of Worm and Worm Gear

The various proportions for worm and worm gear in term of the axial or circular pitch in (mm) are shown in Table 3.

Parameters	Symbol	Single and double threaded
Addendum	a	0.318Pc
Dedendum	d	0.368Pc
Tooth depth	h	0.686Pc
Root diameter of worm	D_{rw}	$D_w - 2D$
Outside diameter of worm	D_{ow}	$D_w + 2a$
Root diameter of worm gear	D_{rg}	$D_g - 0.736P_c$
Outside diameter of worm gear	D_{og}	$D_g + 1.0135P_c$
Throat diameter of worm gear	D_t	$D_g + 0.636P_c$
Radius of gear face	R_f	$0.822P_c + 14$
Radius of gear rim	R_r	$2.2P_c + 14$

Table 3: Proportions for Worm and Worm Gear

The worm and worm gear in mesh is shown in Fig.2.

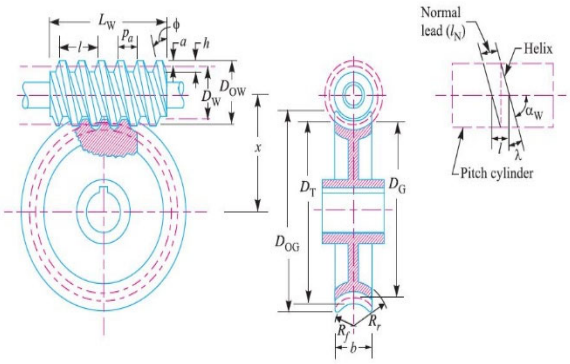


Fig.2. Worm and Worm Gear

Parameters	Symbol	Value	Unit
Addendum	a	1.998	mm
Dedendum	d	2.312	mm
Tooth depth	h	4.310	mm
Root diameter of worm	D_{rw}	17.376	mm
Outside diameter of worm	D_{ow}	25.996	mm
Root diameter of worm gear	D_{rg}	53.376	mm
Outside diameter of worm gear	D_{og}	64.368	mm
Throat diameter of worm gear	D_t	61.996	mm
Radius of gear face	R_f	19.165	mm
Radius of gear rim	R_r	27.823	mm

Table 4: Result Data for Worm and Worm Gear Proportions

2.3. Strength and Dynamic Check of Worm and Worm Gear

In worm gearing, two or more teeth are usually in contact, but due to uncertainty of load distribution among themselves it is assumed that the load is transmitted by one tooth only.

For strength check,

Transmitted torque on worm,

$$T_w = \frac{P \times 60}{2\pi N_w} \quad (14)$$

Actual transmitted tooth load,

$$F_t = \frac{2T_w}{D_w} \quad (15)$$

In the strength check of worm gear tooth, permissible tangential tooth load is calculated by using equation 16.

$$F_T = \sigma_0 C_v b \pi y m_a \quad (16)$$

Where, σ_0 = allowable static stress

C_v = velocity factor

y = Lewis form factor

Allowable static stress σ_0 is 84MPa for phosphor bronze material [3].

Velocity factor,

$$C_v = \frac{6}{6+V_g} \quad (17)$$

Where, V_g = peripheral velocity of worm gear

Peripheral velocity of worm gear,

$$V_g = \frac{\pi D_g N_g}{60} \quad (18)$$

Normal pressure angle ϕ is 14.5°from the range of lead angle λ which is between 0° and 16°. The tooth form factor or Lewis form factor for normal pressure angle ϕ = 14.5° can be calculated by using equation 19.

$$y = 0.124 - \frac{0.684}{n_g} \quad (19)$$

The actual transmitted tooth load is less than the permissible tangential tooth load ($F_t < F_T$), so the design is satisfying.

For dynamics check,

Inaccuracies of the tooth profiles, spacing, misalignment in mounting and tooth deflection under loads result in velocity changes which produce dynamic forces in the gear teeth greater than the transmitted force. The dynamic tooth load is calculated by using equation 20.

$$F_d = \frac{F_t}{C_v} \quad (20)$$

The static tooth load is based on the Lewis equation without a velocity factor. The static tooth load is calculated by using equation 21.

$$F_s = \sigma_e b \pi y m_a \quad (21)$$

Where, σ_e = flexural endurance limit

Flexural endurance limit σ_e is 168MPa for phosphor bronze material.

To insure the durability of a gear pair, the tooth profiles must not have excessive contact stress as determined by wear load. The wear load is calculated by using equation 22.

$$F_w = D_g b K \quad (22)$$

Where, K = load stress factor

Load stress factor K is 0.55MPa for phosphor bronze material.

The dynamics tooth load is less than static tooth load and wear tooth load ($F_d < F_s$, F_w), so the design is satisfying.

Parameters	Symbol	Value	Unit
Actual transmitted tooth load	F_t	269.731	N
Permissible tangential tooth load	F_T	1024.745	N
Dynamics tooth load	F_d	298.045	N
Static tooth load	F_s	2264.631	N
Wear tooth load	F_w	684.383	N

Table 5: Result Data for Strength and Dynamic Check

When the worm gearing is transmitting power, the forces acting on the worm are similar to those on a power screw. Fig.3. shows the forces acting on the worm. The forces on a worm gear are equal in magnitude to that of worm, but opposite in direction as shown in Fig.3.

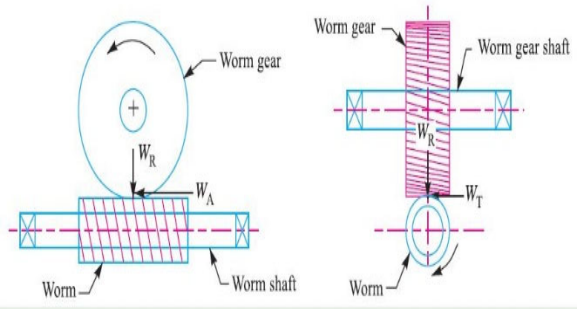


Fig.3. Forces acting on worm teeth

Torque acting on worm gear,

$$T_g = T_w V R \eta \quad (23)$$

The tangential force is the force that acts tangential to the pitch surface of the gear and actually transmits torque and power from the driver to the driving gear. The tangential force on the worm is equal to the axial force on the worm gear is calculated by using equation 24.

$$F_{tw} = F_{ag} = \frac{2T_w}{D_w} \quad (24)$$

The axial force is the force directed parallel to the axis of the shaft carrying the gear. The axial force acting on worm is equal to the tangential force on the worm gear is calculated by using equation 25.

$$F_{aw} = F_{tg} = \frac{2T_g}{D_g} \quad (25)$$

The radial force is the force that acts towards the center of gear. The radial force of worm and worm gear is calculated by using equation 26.

$$F_{rw} = F_{rg} = F_{aw} \tan\phi \quad (26)$$

Parameters	Symbol	Value	Unit
Torque acting on worm	T_w	2.967	Nm
Torque acting on worm gear	T_g	56.007	Nm
Tangential force on worm	F_{tw}	269.727	N
Axial force on worm	F_{aw}	1931.276	N
Radial force on worm	F_{rw}	499.462	N
Tangential force on worm gear	F_{tg}	1931.276	N
Axial force on worm gear	F_{ag}	269.727	N
Radial force on worm gear	F_{rg}	499.462	N

Table 6: Result Data for Forces Acting on Worm and Worm Gear

III. BENDING STRESS ANALYSIS OF WORM GEAR

If the total repetitive load acting on the gear tooth is greater than the beam strength of gear tooth, then the gear tooth will fail in bending. The bending stress of worm gear is calculated by using the following Lewis's bending stress equation 27.

$$\sigma_b = \frac{F_t}{bmY} \quad (27)$$

Shear stress is calculated by using equation 28.

$$\tau_{xy} = \frac{16M_t}{\pi D_g^3} \quad (28)$$

Where, F_t = tangential tooth load
b = face width
m = module
Y = Lewis form factor
M_t = torsional moment
D_g = pitch circle diameter of worm gear

Lewis form factor Y is 0.316for normal pressure angle $\phi = 14.5°$ [5].
The bending stress analysis of worm gear is carried out by varying three different materials. The analysis is conducted to verify the best material for the worm gear in the gear box at higher speed by analyzing stress and strain. The various mechanical properties of the selected materials are given in Table 7.

Mechanical Properties	Phosphor Bronze	Aluminum Bronze	Tin Bronze
Density, ρ (kg/m^3)	8800	7450	8690
Modulus of elasticity, E (GPa)	110	107	103
Poisson ratio, ν	0.341	0.3	0.28
Yield strength, σ_y(MPa)	450	221	172
Ultimate strength, σ_u (MPa)	550	568	241

Table 7: Mechanical Properties of Three Different Materials

Principal stresses,

$$\sigma_{1,2} = \frac{1}{2}(\sigma_x + \sigma_y) \pm \frac{1}{2}\sqrt{(\sigma_x - \sigma_y)^2 + 4\tau_{xy}^2} \quad (29)$$

By using von-Mises criteria,

$$\bar{\sigma} = \frac{1}{\sqrt{2}}\sqrt{(\sigma_1 - \sigma_2)^2 + (\sigma_2 - \sigma_3)^2 + (\sigma_3 - \sigma_1)^2} \quad (30)$$

Principal strain,

$$\varepsilon_1 = \frac{1}{E}[\sigma_1 - \nu(\sigma_2 + \sigma_3)] \quad (31)$$

$$\varepsilon_2 = \frac{1}{E}[\sigma_2 - \nu(\sigma_1 + \sigma_3)] \quad (32)$$

$$\varepsilon_3 = \frac{1}{E}[\sigma_3 - \nu(\sigma_1 + \sigma_2)] \quad (33)$$

Effective strain,

$$\bar{\varepsilon} = \left[\frac{2}{3}(\varepsilon_1^2 + \varepsilon_2^2 + \varepsilon_3^2)\right]^{1/2} \quad (34)$$

IV. NUMERICAL ANALYSIS OF WORM GEAR

The model worm gear is drawn by AutoCAD 2019 software as shown in Fig.4. In this paper, the bending stress of worm gear is calculated by using ANSYS 16.2 software. For this reason, the model of worm gear in AutoCAD 2019 software is exported to ANSYS 16.2 software as an SAT file.

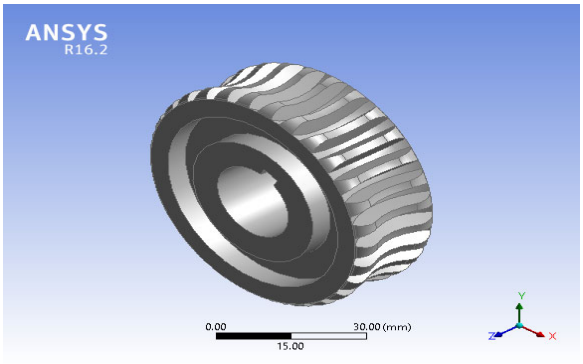


Fig.4. Model of worm gear

This worm geometry model is meshed as shown in Fig.5. This mesh model is imported to static structural analysis.

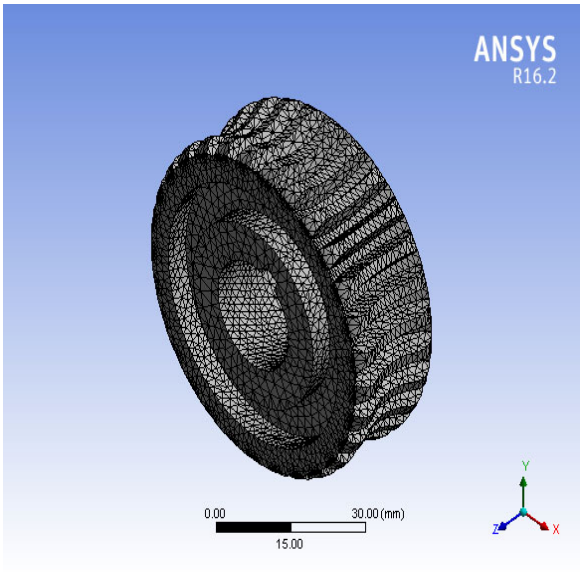


Fig.5. Meshing of worm gear

After applying mesh in a gear teeth, constrain and loading condition are applied on the gear teeth as shown in Fig.6. The fixed support was applied to the inner rim of the worm gear and the torsional moment of 56.007 Nm is applied to the outer rim of the worm gear. And the applied tangential load of 1931.276 N is applied to the root of gear teeth. Boundary condition of worm gear is shown in Fig.6.

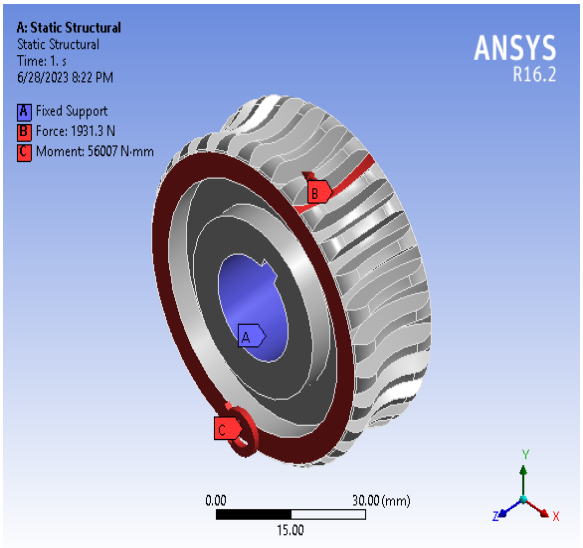


Fig.6. Boundary conditions of worm gear

After meshing and setting up of boundary conditions of worm gear, solved the solution and get equivalent von-Mises stress and effective strain of worm gear. Fig.7. shows the von-Mises stress at the root of worm gear teeth at 132.75 MPa. Fig.8. shows the maximum effective strain of worm gear and the value is 1.363×10^{-3}. And the maximum von-Mises stress and effective strain of worm gear developed by ANSYS 16.2 software are compared with theoretical results.

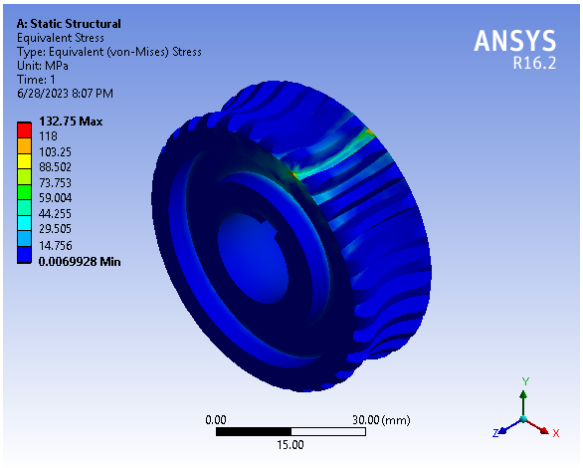


Fig.7. Von-Mises stress of worm gear (phosphor bronze)

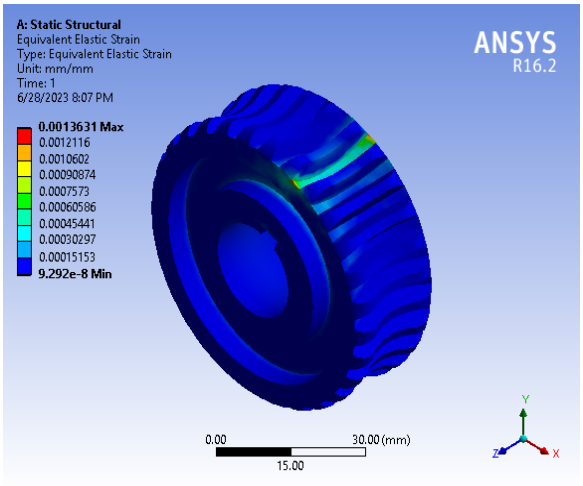


Fig.8. Effective strain of worm gear (phosphor bronze)

The bending stress of worm gear is analyzed by varying three different materials and other parameters are kept constant. Fig.9. shows the simulation result of von-Mises stress for aluminum bronze worm gear. The simulation result of effective strain of worm gear for aluminum bronze is shown in Fig.10.

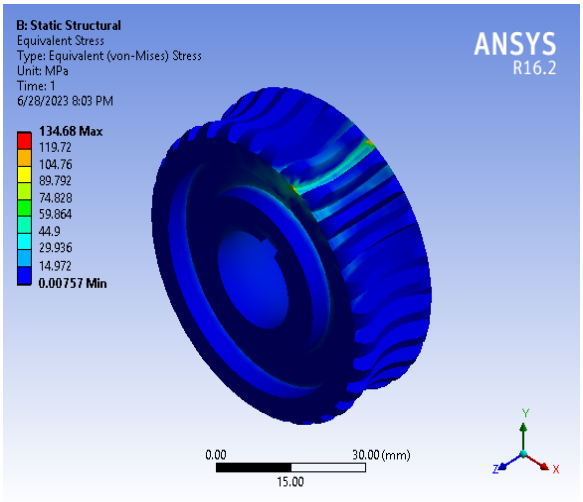


Fig.9. Von-Mises stress of worm gear (aluminum bronze)

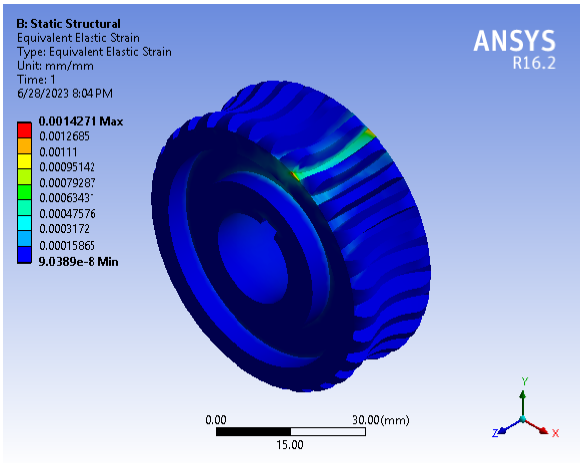


Fig.10. Effective strain of worm gear (aluminum bronze)

The simulation result of von-Mises stress for tin bronze is expressed in Fig.11. The numerical result of effective strain of tin bronze worm gear is shown in Fig.12.

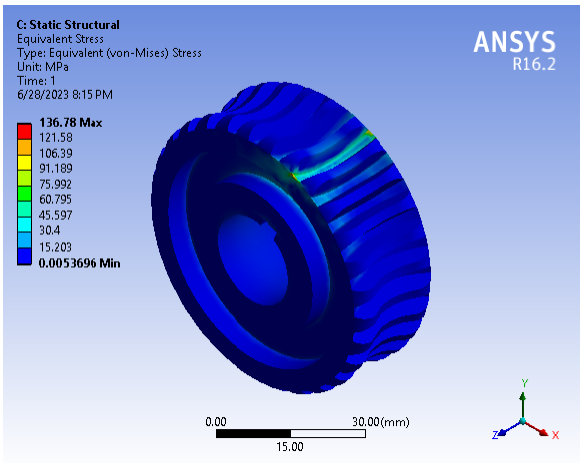


Fig.11. Von-Mises stress of worm gear (tin bronze)

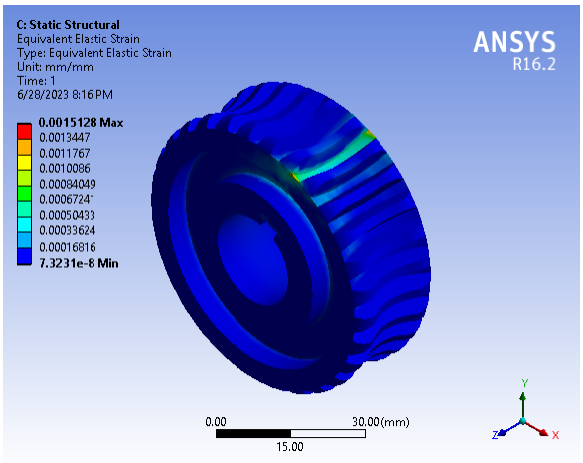


Fig.12. Effective strain of worm gear (tin bronze)

V. RESULT AND DICUSSION

The comparison of von-Mises stress and effective strain of worm gear from theoretical calculations and simulation results are shown in Table 8. In the following Table 8, the comparison between the theoretical and simulation results are nearly the same. So, the design is satisfying.

	Theoretical Result	Numerical Result	Percent Deviation
von-Mises stress (MPa)	142.459	132.750	7%
Effective strain (10^{-3})	1.174	1.363	14%

Table 8: Comparison of von-Mises Stress and Effective Strain for Worm Gear from Theoretical and Simulation Results

The comparison of von-Mises stress values of worm gear with three different materials is expressed in Fig.13. Fig.14. shows the comparison of effective strain of worm gear with three different materials.

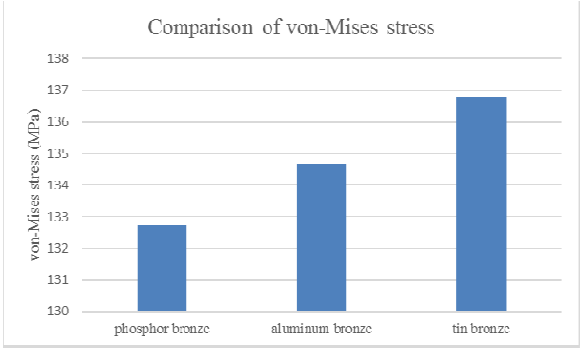


Fig.13. Comparison of von-Mises stress with three different materials

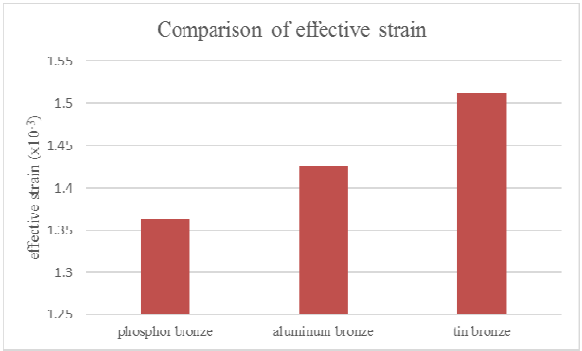


Fig.14. Comparison of effective strain with three different materials

From the above Fig.13. and Fig.14., it was found that the maximum von-Mises stress and effective strain of phosphor bronze are less than other two materials. So, the suitable material for worm gear is phosphor bronze.

VI. CONCLUSION

The design of worm and worm gear are designed for transmission system of mini power weeder. For strength check of worm gear, the actual transmitted load is determined from transmitted torque. The tooth load is less than permissible tooth load. Therefore, strength check is satisfying. All gear teeth of

transmission gear have sufficient strength and they are not failure under static loading and dynamics loading. So, the static tooth load and wear load are greater than dynamics tooth load. So, dynamics check is satisfactory.In structural analysis of worm gear, the structural behaviors are calculated by theoretically and numerically. The numerical von-Mises stress and effective strain of worm gear are done with three different materials and are chosen the suitable material. The von-Mises stress of phosphor bronze, aluminum bronze, and tin bronze are 132.75, 134.68, and 136.78 MPa. The effective strain of three materials are 0.0013631, 0.0014271, and 0.0015128. So, phosphor bronze is suitable for worm gear.

ACKNOWLEDGMENTS

The author would like to thank to Farm Machinery Factory, Mandalay Industrial Zone for their help with permission to be able to collect the required data for mini power weeder worm gear and Head of Departmentand all teachers from Mechanical Engineering Department for their kind supervision, encouragement, suggestion, and valuable guidelines for this paper.

REFERENCES

[1] Faydor L. Litvin, Alesssandro Nava, “New geometry of face worm gear drives with conical and cylindrical worms: generation, simulation of meshing, and stress analysis”, 2002.

[2] A.H. Falah, “Load and Stress Analysis of Cylindrical Worm Gear Using Tooth Slicing Method”, 2005.

[3] R.S. Khurmi, J.K. Gupta, “A textbook of Machine Design”, 2005.

[4] Y.K. Mogal, “A Multi-objective Optimization Approach for Design of Worm and Worm Wheel based on Genetic Algorithm”, 2013.

[5] Richard G. Budynas, J. Keith Nisbett, “Mechanical Engineering Design Tenth Edition”, 2015.

[6] Yuvraj B. Jadhava, “Mathematically modelling and design of worm and worm gear for determining the surface stress acting on the tooth of worm and worm gear for plug valve application”, vol.8, Issue-4, ISSN:2229-5518, 2017.

[7] Anand Mohan Singh, MeghaBhawsar, Neeraj Kumar Nagayach, “Structure Analysis, Contact Stress Analysis and Fatigue Life Analysis of Spur Gear Assembly by Using Fem”, vol.4, Issue-4, ISSN:2455-0108, 2018.

[8] May Phyoe Thu, “Stress Analysis on Spur Gears Using ANSYS Workbench 16.0”, vol.7, Issue-08, ISSN:2319-7560, 2018.

[9] Rufus O. Chime, “Design, modeling, simulation of worm gears: analysis of worm gears”, vol.5, Issue-5, ISSN:2319-5967, 2018.

★★★